

# Measuring vitamin B-12 bioavailability with [<sup>13</sup>C]-cyanocobalamin in humans

Sarita Devi,<sup>1</sup> Roshni M Pasanna,<sup>1</sup> Zeeshan Shamsuddin,<sup>1</sup> Kishor Bhat,<sup>1</sup> Ambily Sivasdas,<sup>1</sup> Amit K Mandal,<sup>2</sup> and Anura V Kurpad<sup>3</sup>

<sup>1</sup>Division of Nutrition, St. John's Research Institute, St. John's National Academy of Health Sciences, Bangalore, India; <sup>2</sup>Division of Clinical Proteomics, St. John's Research Institute, St. John's National Academy of Health Sciences, Bangalore, India; and <sup>3</sup>Department of Physiology, St. John's Medical College, St. John's National Academy of Health Sciences, Bangalore, India

## ABSTRACT

**Background:** Vitamin B-12 deficiency is widespread in many parts of the world, affecting all age groups and increasing with age. It is primarily due to a low intake of animal source foods or malabsorption. The measurement of bioavailability of vitamin B-12 is etiologically important in deficiency but is limited due to the use of radioactive isotopes like [<sup>57</sup>Co]- or [<sup>14</sup>C]-cyanocobalamin.

**Objectives:** The aim of this study was to measure the bioavailability of [<sup>13</sup>C]-cyanocobalamin in humans and to assess the effect of parenteral replenishment of vitamin B-12 on the bioavailability.

**Methods:** We synthesized a stable isotope-labeled vitamin B-12, [<sup>13</sup>C]-cyanocobalamin, using *Salmonella enterica* by providing [<sup>13</sup>C<sub>2</sub>]-ethanolamine as a sole carbon source. After purification and mass spectrometry-based characterization, its oral bioavailability was measured in the fasted state with high and low oral doses, before and after parenteral replenishment of vitamin B-12 stores, from the kinetics of its plasma appearance in a 2-compartment model.

**Results:** [<sup>13</sup>C]-cyanocobalamin was completely decyanated to [<sup>13</sup>C]-methylcobalamin describing metabolic utilization, and its plasma appearance showed early and late absorption phases. At a low dose of 2.3 μg, the mean bioavailability was 46.2 ± 12.8 (%), mean ± SD, *n* = 11). At a higher dose of 18.3 μg, the mean bioavailability was 7.6 ± 1.7 (%), mean ± SD, *n* = 4). Parenteral replenishment of the vitamin B-12 store in deficient individuals prior to the measurement resulted in a 1.9-fold increase in bioavailability.

**Conclusions:** Vitamin B-12 bioavailability is dose dependent and at a low dose that approximates the normal daily requirement (46%). The stable isotope method described here could be used to define the etiology of deficiency and to inform the dietary requirement in different physiologic states as well as the dose required for supplementation and food fortification. This trial was registered at the Clinical Trials Registry of India as CTRI/2018/04/012957. *Am J Clin Nutr* 2020;112:1504–1515.

**Keywords:** vitamin B-12, stable isotope, bioavailability, mass spectrometry, cyanocobalamin, methylcobalamin, biosynthesis, human, pharmacokinetics

## Introduction

The measurement of vitamin B-12 absorption by the Schilling test (1, 2), using an oral dose of [<sup>57</sup>Co]-cyanocobalamin, is difficult to perform in healthy subjects today due to restrictions on the general use of radioisotopes. Measuring vitamin B-12 bioavailability is particularly important in many countries, including India, where vitamin B-12 intake is low (3) with respect to the suggested daily requirement of 2.4 to 4 μg/d (4), leading to widespread deficiency in the population, including pregnant women (5, 6). *Helicobacter pylori* infection (7) and

Data described in the manuscript, code book, and analytic code will be made available upon reasonable request to the corresponding author.

**Funding:** This research was supported by the Indian Department of Biotechnology (grant BT/PR13918/PFN/20/1033/2015) and by the Wellcome Trust/DBT India Alliance Margdarshi Fellowship (No. IA/M/14/1/501681) awarded to AVK.

ZS: Present address: Biocon Research Limited, Bangalore, India.

AKM: Present address: Department of Biological Sciences, Indian Institute of Science Education and Research, Kolkata, India.

Supplemental methods, Supplemental Tables 1 and 2 and Supplemental Figures 1–13 are available from the “Supplementary data” link in the online posting of the article and from the same link in the online table of contents at <https://academic.oup.com/ajcn/>.

Address correspondence to AVK (e-mail: [a.kurpad@sjri.res.in](mailto:a.kurpad@sjri.res.in)).

Abbreviations used: ALA, aminolevulinic acid; DMB, dimethylbenzimidazole; HoloTC, holotranscobalamin; Hcy, homocysteine; HRAM, high-resolution accurate mass spectrometry; IMMC, interdigestive migrating motility complex; IS, internal standard; LB, Luria-Bertani; MMA, methylmalonic acid; MALDI-MS, matrix-assisted laser desorption/ionization mass spectrometry; SAEM, stochastic approximation expectation maximization.

**Disclaimer:** Corresponding author is an associate editor with *AJCN*. The part of this research work was presented at ASN conference (2020) and published in *Current Developments in Nutrition*.

Received March 20, 2020. Accepted for publication July 10, 2020.

First published online August 25, 2020; doi: <https://doi.org/10.1093/ajcn/nqaa221>.

the widespread use of drugs such as proton-pump inhibitors and metformin also increase the risk of deficiency (8). The elderly are also at high risk of developing B-12 deficiency due to malabsorption of food-bound cobalamin caused by atrophic gastritis (9, 10). Oral vitamin B-12 supplementation shows a marked interindividual heterogeneity in response, possibly related to variable bioavailability, which is also dependent on the gastrointestinal absorption (11). Here, bioavailability refers to the appearance of intestinally absorbed vitamin B-12 in the plasma after first pass through the liver and in relation to its distribution into the body tissue pool and elimination.

The Schilling test uses a 2-stage procedure, where [ $^{57}\text{Co}$ ]-cyanocobalamin is orally administered followed by a flushing dose of nonlabeled vitamin B-12 administered intramuscularly, to force the urinary excretion of the administered radiolabeled vitamin B-12 in 24 h (1, 2). The egg-yolk cobalamin absorption test, which is a modification of the Schilling's test, also administers [ $^{57}\text{Co}$ ]-vitamin B-12 along with albumin, egg yolk, or chicken in a similar protocol (12, 13). An alternative is to use [ $^{14}\text{C}$ ]-vitamin B-12 (cyanocobalamin) (14), which poses negligible radiation risk to the subject compared with [ $^{57}\text{Co}$ ] and is performed without a flushing dose of vitamin B-12 and without 24-h urine collection. Although indirect indicative methods such as the use of plasma holotranscobalamin (HoloTC) concentration, also known as active B-12, have been developed to estimate the fractional absorption of vitamin B-12 (15), there is still no direct, completely safe, nonradioactive method for determining vitamin B-12 bioavailability. In this study, we aimed to biosynthesize quantitatively significant amounts of [ $^{13}\text{C}$ ]-cyanocobalamin from *Salmonella enterica*, followed by the measurement of its bioavailability in human subjects at low and high doses, as well as the influence of the body vitamin B-12 store on bioavailability.

## Methods

### Biosynthesis, characterization, and safety of [ $^{13}\text{C}$ ]-cyanocobalamin

The bacterial strain *S. enterica* (serovar Typhimurium) strain TT24733, genotype *cbiD24::MudJ* was precultured in sterile Luria-Bertani (LB; HIMEDIA) medium (10 g peptone, 5 g yeast extract, and 10 g NaCl) and cryopreserved using DMSO (Sigma-Aldrich). For culture initiation, an aliquot was thawed and 100  $\mu\text{L}$  was added to 5 mL LB medium and incubated for 12 h at 37°C in a shaker incubator at 250 rpm. After incubation, the culture was streaked onto sterile LB agar plates and incubated at 37°C to obtain single distinct colonies that were further grown on NCE medium (No Carbon E). The detailed method for biosynthesis and purification of [ $^{13}\text{C}$ ]-cyanocobalamin is described in the supplemental methods. Once the synthesized [ $^{13}\text{C}$ ]-cyanocobalamin was characterized by matrix-assisted laser desorption/ionization mass spectrometry (MALDI-MS), the pilot cultures were then scaled to larger batch cultures for higher yields and quantified by semipreparative high-performance liquid chromatography (LC) (see **Supplemental methods** for details). To examine its safety, the purified [ $^{13}\text{C}$ ]-cyanocobalamin was orally dosed in the morning to Wistar rats ( $n = 2$ , 1.2 mg) after withholding food for 1 night. About 2 h after the dose, normal feeding was allowed. The rats were observed for their behavior

(posture, activity, and sleep) and any morbidity. They remained normal and active during the observation period, and no adverse events were noted up to 3 mo after dosing. This study protocol was approved by the Institutional Animal Ethical Review Board of St. John's Medical College, Bengaluru, India.

### Human vitamin B-12 absorption protocols

The bioavailability of [ $^{13}\text{C}$ ]-cyanocobalamin was measured in healthy adults (aged 20–40 y) with a BMI <25 (in  $\text{kg}/\text{m}^2$ ). The CONSORT flowchart demonstrating the subject recruitment procedure is described in **Supplemental Figure 1**. The Institutional Ethical Review Board of St. John's Medical College, Bengaluru, India, approved the study protocols, and written informed consent was obtained from all the subjects at enrollment. The study was registered at the Clinical Trials Registry of India as CTRI/2018/04/012957.

At screening, the subjects underwent a full clinical examination, followed by testing of their complete blood count (ABX Pentra 60 C+; HORIBA ABX Diagnostics) and plasma total vitamin B-12 (Siemens Advia XPT immunoassay platform) and active B-12 (HoloTC; Abbott Architect Analyzer) concentration. Biorad Lyphochek trilevel immunoassay quality controls were used and inter- and intra-assay CVs were 8.0% and 5.0%, respectively. The combined measurement of plasma methylmalonic acid (MMA) and homocysteine (Hcy) concentrations was analyzed by gas chromatography mass spectrometry (GCMS-SQ, 5975; Agilent Technologies). An aliquot of 200  $\mu\text{L}$  samples and pooled quality control samples were treated with dithioerythritol (20  $\mu\text{L}$ ; 200 mmol/L) containing a mixture of  $\text{d}_8$ -homocystine (DL-[3,3,3',3',4,4,4',4'- $^2\text{H}_8$ ] and  $\text{d}_3$ -MMA, >98% purity; Cambridge Isotope Laboratories) as an internal standard and converted to their *N(S)*-methoxycarbonyl ethyl esters (16). The intra-assay CVs were <4% and <2% and interassay CVs were <6% and <3% for MMA and Hcy, respectively.

### Pharmacokinetics of a high oral dose (18.3 $\mu\text{g}$ ) of [ $^{13}\text{C}$ ]-cyanocobalamin.

Healthy young subjects were studied to understand and characterize [ $^{13}\text{C}$ ]-cyanocobalamin kinetics at a higher dose (~10 times) than the daily vitamin B-12 requirement (17, 18). This was needed for evaluating and selecting an appropriate compartmental pharmacokinetic model for further use with lower doses that mimicked the daily requirement. Briefly, all subjects ( $n = 4$ ; 2 males, 2 females) reported at the metabolic ward of St. John's Medical College at 06:00 on the experimental day. After their height (Seca) and weight (Goldtech) were measured, an intravenous catheter (Jelco 22 G; Medex Medical Ltd) was inserted into the antecubital vein. A baseline blood sample was collected, following which the subjects were orally administered with a [ $^{13}\text{C}$ ]-cyanocobalamin (18.3  $\mu\text{g}$ ) dose dissolved in distilled water (2 mL), followed by a chaser of 100 mL distilled water. The dose was gravimetrically prepared on a standard weighing scale (Sartorius). The subjects were allowed to have water ad libitum thereafter, with a light meal offered between the 6th and 7th h after dosing. Blood samples were collected hourly through the 12 h after the dose administration and daily at ~09:00 thereafter, until the 5th day after the dose. Blood samples were protected

from light by collection in aluminum foil-wrapped EDTA-coated vacutainers (Becton Dickinson) and processed for plasma separation immediately by centrifugation (5810 R; Eppendorf) at 2588 g for 10 min at 4°C and stored in amber vials at -80°C.

#### ***Pharmacokinetics of a low oral dose (2.3 µg) of [<sup>13</sup>C]-cyanocobalamin.***

Healthy male subjects ( $n = 11$ ) were studied for vitamin B-12 bioavailability at the daily requirement dose by administering [<sup>13</sup>C]-cyanocobalamin at around the recommended dietary intake of 2.5 µg (17). One of the subjects from the high-dose experiment took part in this experiment as well; the 2 tests in this subject were separated by more than 2 mo. A baseline blood sample was collected at the beginning of the experiment and subjects were orally administered with a [<sup>13</sup>C]-cyanocobalamin (2.3 µg) dose along with distilled water. The subjects were allowed to have water ad libitum thereafter, with a light meal offered between the 6th and 7th h after dosing. The experimental protocol was similar to the high-dose pharmacokinetics study as described above, except that in this experiment, the subjects were studied for only 12 h with hourly blood collection. This time frame was selected because the earlier high-dose experiment showed that the peak maxima was at about 5–8 h, followed by a decline in the next few hours, which plateaued over the next few days. From the viewpoint of a practical human bioavailability study, it was deemed to be adequate for the purpose of measuring bioavailability from a single dose.

#### ***Pharmacokinetics of a low oral dose (2.3 µg) of [<sup>13</sup>C]-cyanocobalamin after replenishing vitamin B-12 stores in subjects with low vitamin B-12 status.***

Since the elimination of absorbed vitamin B-12 from the plasma includes transfer into tissue pools, an increase in this transfer parameter in vitamin B-12-deficient subjects (with lower tissue pool size) could result in an apparently low bioavailability as judged from the pharmacokinetic model. Therefore, repeat measurements were made in 3 subjects from the low oral dose experiment who had apparently low vitamin B-12 status as shown by their plasma active B-12 (HoloTC) concentrations (<30 pmol/L). Here, [<sup>13</sup>C]-cyanocobalamin bioavailability was reassessed after the replenishment of their body vitamin B-12 status by the intramuscular injection of 1 mg hydroxocobalamin (Trineurosol-Hp; Zen Pharma Pvt Ltd). The reassessment of bioavailability of [<sup>13</sup>C]-cyanocobalamin was performed within 2 wk of this replenishment. All other experimental procedures were similar to those described earlier.

#### **Sample preparation and high-resolution accurate mass analysis for quantitative profiling of cyano-, methyl-, hydroxo-, and adenosylcobalamin**

Plasma samples (1 mL) were spiked with 10 µL internal standard (IS; methotrexate, 0.20 µmol/L; Sigma-Aldrich) and vortex mixed for 10 s, followed by acidification by the addition of 175 µL formic acid before deproteinization. A 4-fold of chilled

organic solvent [100% acetonitrile, liquid chromatography mass spectrometry (LCMS) grade; Honeywell] was added to each sample, vortexed vigorously, and kept at 4°C for 10 min, followed by centrifugation (5810 R; Eppendorf) at 15,294 g for 30 min at 4°C. Acidified supernatants were dried in a vacuum concentrator (Labconco) at 30°C for 7 h. All sample preparation was done in the dark. Dried samples were reconstituted in 200 µL water, and analysis was performed on a high-resolution analytical platform consisting of a Vanquish Flex Binary UHPLC coupled to a mass spectrometer (Q Exactive, LC-HRAM-MS; Thermo Scientific) with a heated electrospray ionization (HESI-II) probe. Separation of the different forms of vitamin B-12 (hydroxo, cyano, ado, and methyl) was achieved by using a Hypersil Gold aQ column (100 × 2.1 × 1.9 µm; Thermo Scientific). The mobile phase was delivered in a reversed-phase gradient elution at 0.3 mL/min, using water (eluent A) and acetonitrile (eluent B), both containing 0.1% formic acid. The following gradient profile was used: 5% B at 0–2 min and increased to 50% B in 22 min and then increased to 98% B at 23 min and held for 2 min and then decreased to 5% B at 26 min and equilibrated for another 7 min. The column temperature was maintained at 40°C, and injection volume was 50 µL for each of the solvent blanks, standards, and samples.

The MS was operated in heated-electrospray mode with positive polarity in a parallel reaction monitoring method, with normalized collision energy of 35 and 2 microscans at 17,500 resolution with automatic gain control target of  $5e^4$  ions and a maximum ion injection time of 80 ms with the isolation window set at 4.0  $m/z$ . Source parameters were as follows: sheath gas flow rate, 40; auxiliary gas flow rate, 10; spray voltage, 4.0 kV; capillary temperature, 330°C; heater temperature, 350°C; and S-Lens RF level 60. The data were acquired by using Thermo Scientific Xcalibur software (Version 4.1.31.9). Doubly charged species for cyano-, methyl-, hydroxo-, and adenosylcobalamin (Figure 1) were used for quantification. The precursor (product ions) masses monitored were 678.29098 (147.09164, 912.44135) and 680.29738 (147.09164, 914.44135), 672.80149 (147.09164, 971.47383) and 674.80149 (147.09164, 973.47383), 664.78568 (147.09174, 912.44165) and 666.78568 (147.09174, 914.44165), and 790.33645 (147.09165, 971.47968) and 792.33645 (147.09164, 973.47968) for [<sup>12</sup>C]- and [<sup>13</sup>C]-cobalamin species for cyano-, methyl-, hydroxo- and adenosylcobalamin, respectively, and 455.17859 (134.06004, 175.07263, 308.12527) for methotrexate. Standard curves were linear in the range of 50–2000 pmol/L for cyano-, methyl-, hydroxo-, and adenosylcobalamin ( $r^2 = 0.9979$ ) and reproducibility (CV <8%). The peak-area ratios of the respective cobalamins to the IS were plotted against their concentrations. The concentrations of unknown samples were calculated from the respective regression equations for individual cobalamin forms. Intra- and interassay CVs were <6% and <8% respectively.

#### **Mathematical model for bioavailability**

We used plasma concentration data from the high-dose experiment to define the structure of the kinetic model since these would have a high signal-to-noise ratio, and the subjects were followed up for an adequately long period (days) after the dose. While cyanocobalamin gets metabolized to other active vitamin B-12

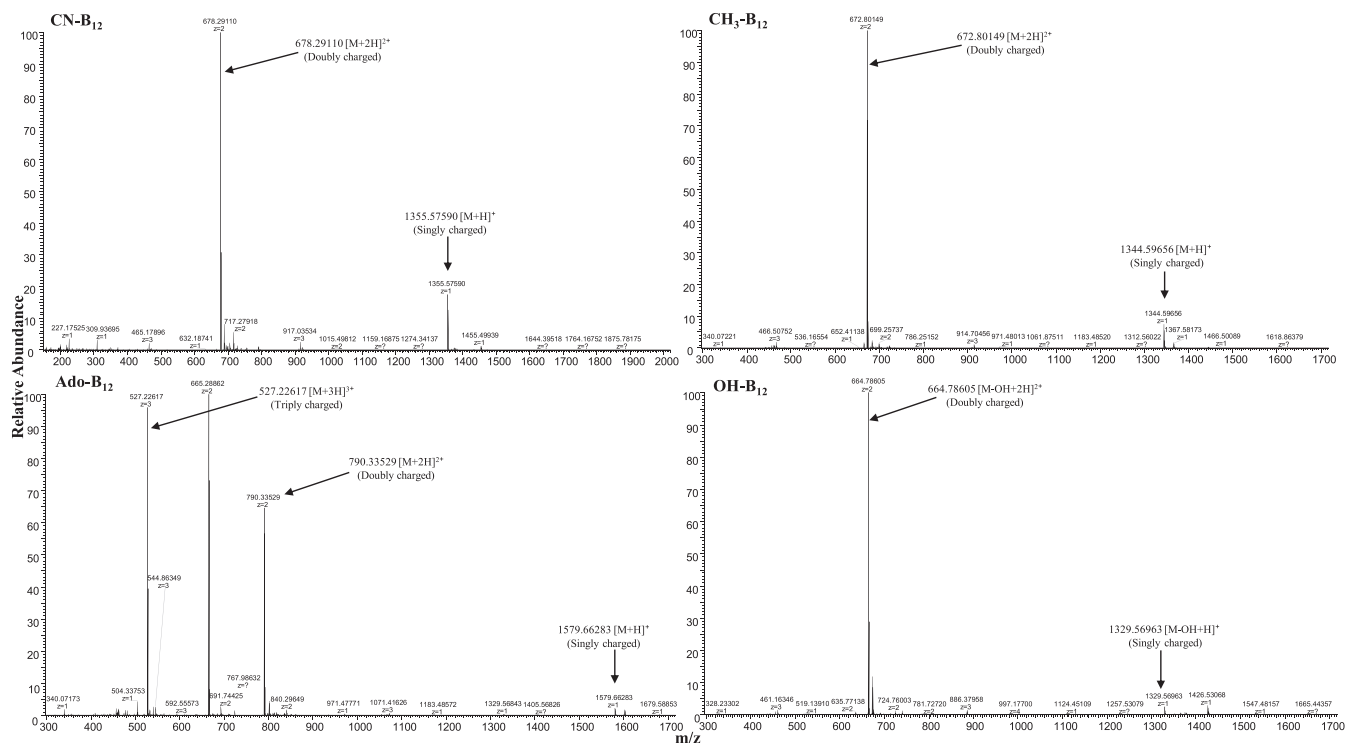


**FIGURE 1** High-resolution accurate mass spectrometry analysis of CN (cyano), Ado (adenosyl), CH<sub>3</sub> (methyl), and OH (hydroxo)- vitamin B-12 (singly, doubly, and triply charged species). The precursor masses at  $m/z$  678.29098 and  $m/z$  680.29738,  $m/z$  672.80149 and  $m/z$  674.80149,  $m/z$  664.78568 and  $m/z$  666.78568, and  $m/z$  790.33645 and  $m/z$  792.33645 for [<sup>12</sup>C]- and [<sup>13</sup>C]-cobalamin species of cyano-, methyl-, hydroxo-, and adenosylcobalamin, respectively.

forms (methylcobalamin and adenosylcobalamin) that appear in the plasma after decyanation (19), only [<sup>13</sup>C]-methylcobalamin was observed in the plasma after the administration of oral [<sup>13</sup>C]-cyanocobalamin to the subjects. Therefore, we used only serial plasma [<sup>13</sup>C]-methylcobalamin concentrations for the mathematical model.

As vitamin B-12 absorption saturates at doses above 1.5  $\mu\text{g}$  (20), absorption was modeled as zero-order processes. Visual inspection of the plasma appearance of [<sup>13</sup>C]-methylcobalamin concentrations following an oral administration of a high dose (18.3  $\mu\text{g}$ ) of [<sup>13</sup>C]-cyanocobalamin revealed complex and variable concentration-time profiles, characterized by an early small peak preceding the classically described absorption peak between 5 and 12 h (14) after the ingestion of dose (Figure 2A). Therefore, we modeled bioavailability as a function with 2 independent zero-order components with a time lag corresponding to the second phase of absorption. A fraction of the bioavailable dose ( $F_1$ ) was absorbed in a zero-order process at a constant rate for a time period ( $Tk_{01}$ ) without any delay, while the remaining fraction was absorbed after a nonzero lag time ( $Tlag_2$ ) by another zero-order mechanism over a specific time duration ( $Tk_{02}$ ). These 2 phases could be interpreted as due to classical active absorption in the ileum in the second phase but also a mix of passive absorption in the upper gut and a component of early active absorption due to rapid gastric emptying and small intestinal transit in the first phase. Our model also assumed a core compartment (pool) by way of the plasma and a peripheral compartment, which corresponded to tissue (Figure 2B). The description of the mathematical model used is

described in detail in supplemental methods and **Supplemental Table 1**.

Population pharmacokinetic parameters were estimated by maximum likelihood, using the stochastic approximation expectation maximization (SAEM) algorithm without any model approximation (no linearization). The between-subject variabilities (BSVs) for all parameters were estimated assuming a log-normal distribution except for the use of logit distribution for the fraction of the double absorption ( $F_1$ ) parameter. A combined proportional and additive model was used to describe residual variability. Parameter stability and convergence were evaluated using the Monolix assessment suite (at default settings) with 5 SAEM parameterizations of random initial parameter values uniformly drawn from intervals defined around all the final population estimates. Log-likelihood estimation was performed by importance sampling, where a fixed  $t$  distribution is assumed with 5 degrees of freedom. The selection of covariates is described in the supplemental methods.

### Statistical analyses

Data are presented as means and SDs. Pearson correlations were performed when data were normally distributed; if not, Spearman correlation was performed to evaluate associations between the absorption data and indices such as plasma HoloTC (active B-12), which is considered an indirect measure of vitamin B-12 absorption (21), as well as other biomarkers of vitamin B-12 status, such as plasma homocysteine and

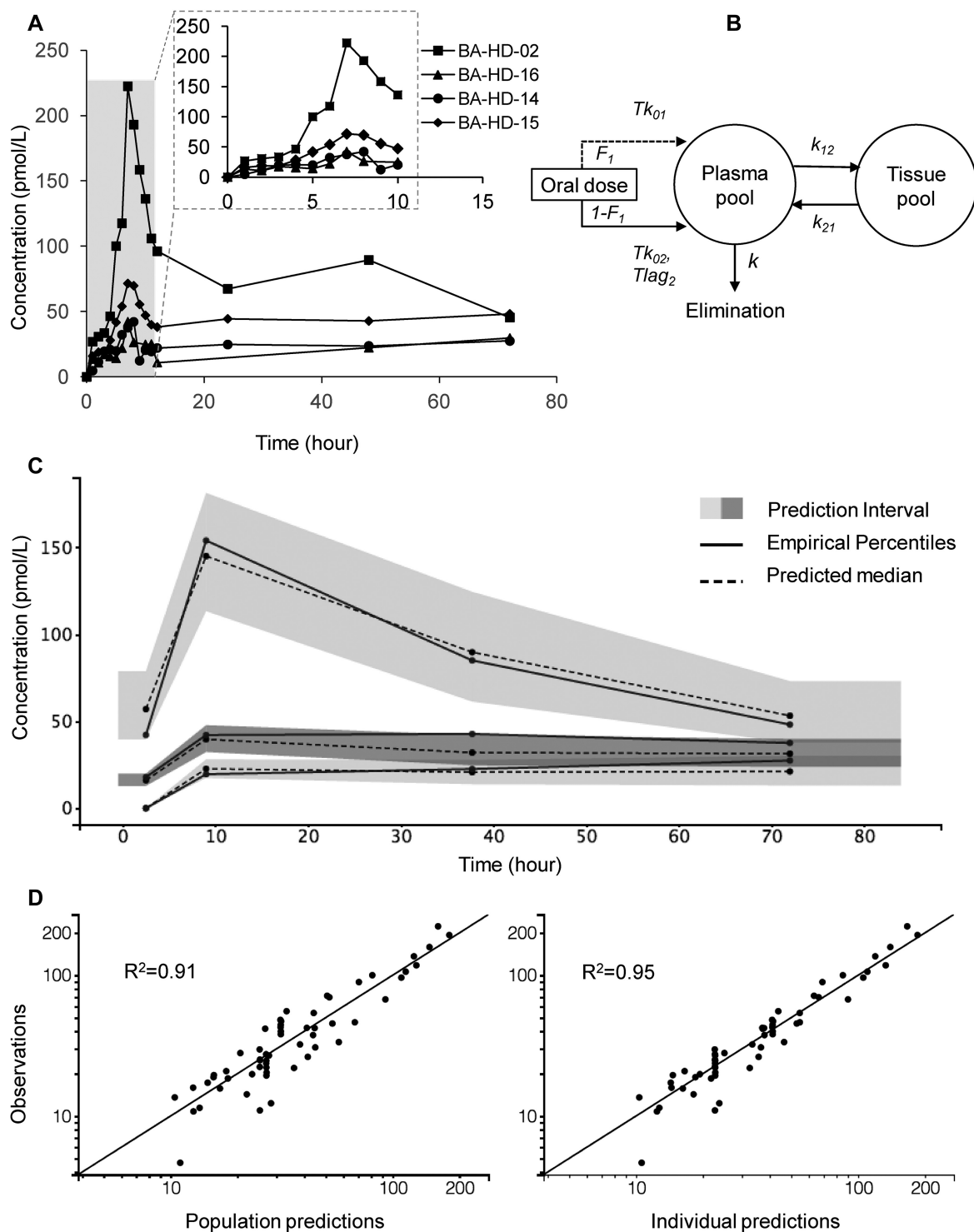


**FIGURE 2** Subject-specific [ $^{13}\text{C}$ ]-methylcobalamin concentration-time profiles in a high-dose experiment along with schematic description of the kinetic model and goodness-of-fit plots. (A) Subject specific [ $^{13}\text{C}$ ]-methylcobalamin concentration-time profiles in healthy subjects after oral administration of a high dose of [ $^{13}\text{C}$ ]-cyanocobalamin (mean dose = 18.3  $\mu\text{g}$ ) that indicates more than 1 absorption phase involving delays. (B) Tissue pool represents body tissue storage pool. Clearance represents elimination from the plasma pool due to renal excretion or irreversible tissue (cellular) utilization.  $(1 - F_1)$ , the remaining fraction of the bioavailable dose absorbed by the second zero-order process;  $F_1$ , fraction of the bioavailable dose absorbed by the first zero-order mechanism;  $k$ , elimination rate constant;  $k_{12}$ , distribution rate constant from compartment 1 (plasma) to compartment 2 (peripheral tissue);  $k_{21}$ , distribution rate constant from compartment 2 (peripheral tissue) to compartment 1 (plasma);  $Tk_{01}$ , duration of the first zero-order process;  $Tk_{02}$ , duration of the second zero-order process;  $Tlag_2$ , time delay before the start of the second zero-order absorption process. (C) Visual predictive check plot of the chosen model that describes the concentration-time profiles of individuals in the high-dose experiment. The 10th, 50th, and 90th empirical percentiles are depicted. Predictions are based on 500 simulations of the data set using the final pharmacokinetic parameter estimates. (D) Scatterplots of the observed concentrations compared with the population model predictions (left) and the individual model predictions (right).

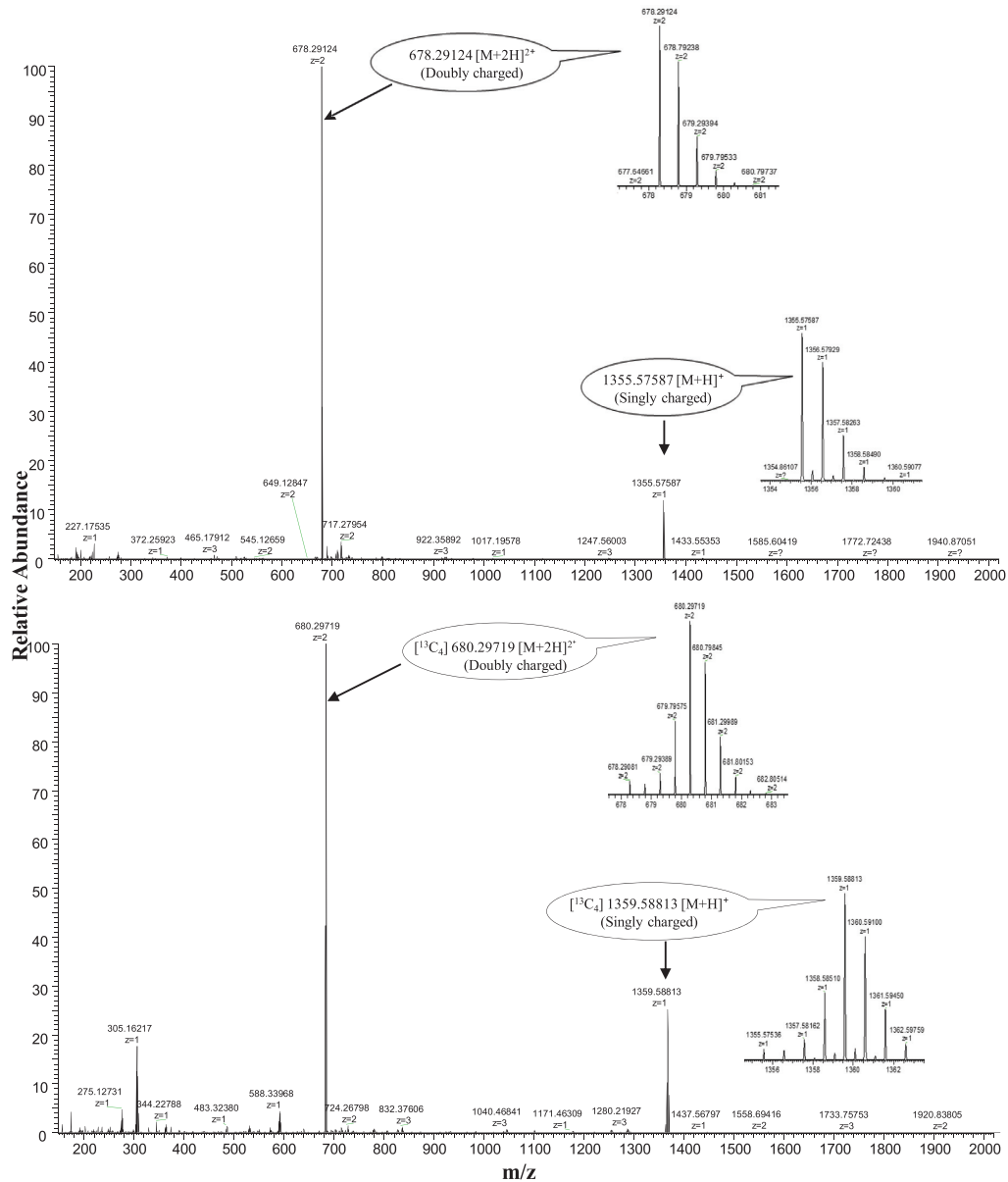


**FIGURE 3** High-resolution accurate mass spectrometry analysis of the synthesized  $[^{13}\text{C}]$ -cyanocobalamin showing doubly charged ion at  $m/z$  680.29768  $[\text{M} + 2\text{H}]^{2+}$  with the 4-Dalton shift as compared with standard cyanocobalamin.

methylmalonic acid. Correlations of absorption and vitamin B-12 status (plasma vitamin B-12 and HoloTC concentrations) were performed for absorption in the low-dose  $[^{13}\text{C}]$ -cyanocobalamin and for pooled data from all subjects, including those after vitamin B-12 replenishment, respectively. A nonlinear mixed-effect modeling software, Monolix 2019R2 (Lixoft), was used to perform analyses.  $P < 0.05$  was considered statistically significant. To develop a simple protocol for clinical testing, where the blood sampling burden on the subject is reduced to 1 or 2 postdose samples, the measured bioavailability was correlated with the plasma  $[^{13}\text{C}]$ -methylcobalamin concentration at different time points (5–8 h after the dose) around the observed peak values. The time points at which the best correlation of plasma  $[^{13}\text{C}]$ -methylcobalamin concentration with bioavailability were observed are reported.

## Results

### Mass spectrometry characterization of synthesized $[^{13}\text{C}]$ -cyanocobalamin

The large-scale batch cultures yielded ~30 mg of purified  $[^{13}\text{C}]$ -cyanocobalamin, which was stored for further animal and human experiments. The LC profile and UV absorption spectrum of synthesized  $[^{13}\text{C}]$ -cyanocobalamin are provided in **Supplemental Figure 2A** and **B**. The MALDI-MS profile and structural representation of  $[^{13}\text{C}]$  incorporation are provided in **Supplemental Figures 3** and **4**. High-resolution accurate mass spectrometry (HRAM) analysis of the pooled large-scale batch cultures showed a doubly charged ion at  $m/z$  680.29719  $[\text{M} + 2\text{H}]^{2+}$  as the most intense peak with the 4-Dalton shift for  $[^{13}\text{C}]$ -cyanocobalamin compared with standard cyanocobalamin

**TABLE 1** Anthropometric and biochemical parameters of the subjects in the high-dose ( $n = 4$ ; 2 males and 2 females) and low-dose ( $n = 11$ ; males) [ $^{13}\text{C}$ ]-cyanocobalamin experiments<sup>1</sup>

Variable	High dose	Low dose
Age, y	28.0 $\pm$ 4.4	26.8 $\pm$ 6.7
Weight, kg	59.1 $\pm$ 13.3	67.6 $\pm$ 7.8
Height, m	1.7 $\pm$ 0.1	1.7 $\pm$ 0.1
BMI, kg/m <sup>2</sup>	21.3 $\pm$ 1.4	23.6 $\pm$ 2.8
Hb, g/dL	14.2 $\pm$ 0.7	14.9 $\pm$ 1.2
Vitamin B-12, pmol/L	269.2 $\pm$ 211	196.6 $\pm$ 56
HoloTC, pmol/L	47.9 $\pm$ 53.6	36.8 $\pm$ 20.2

<sup>1</sup>Values are represented as mean  $\pm$  SD. Hb, hemoglobin; HoloTC, holotranscobalamin.

(Figure 3), which was chosen for the quantification and bioavailability estimations. The purity of the synthesized [ $^{13}\text{C}$ ]-cyanocobalamin was >98%, as computed by the relative mass distributions of each of the doubly and singly charged [ $^{13}\text{C}$ ] species to its natural [ $^{12}\text{C}$ ] form.

### Human vitamin B-12 bioavailability protocols

#### Pharmacokinetics of a high oral dose (18.3 $\mu\text{g}$ ) of [ $^{13}\text{C}$ ]-cyanocobalamin.

The anthropometric and biochemical data of the study participants ( $n = 4$ ; 2 males and 2 females) are provided in Table 1. All subjects had a BMI of 18.5–25, and their plasma vitamin B-12 concentrations were within the reference range (>150 pmol/L).

All the orally administered [ $^{13}\text{C}$ ]-cyanocobalamin was converted to circulating [ $^{13}\text{C}$ ]-methylcobalamin, as the other forms (hydroxocobalamin, adenosylcobalamin, and the administered cyanocobalamin) were undetectable at all sampling points. Therefore, the serial plasma [ $^{13}\text{C}$ ]-methylcobalamin concentrations were used for developing a population pharmacokinetic model based on a 2-compartment model with plasma and tissue pools along with linear elimination from the plasma pool in the form of renal clearance and irreversible tissue utilization. The subject-specific appearance of [ $^{13}\text{C}$ ]-methylcobalamin concentrations is shown in Figure 2A and Supplemental Figure 5. A 2-phase absorption model involving an early zero-order absorption process along with a delayed zero-order absorption phase was used to describe the double-peak phenomenon observed in the data. A schematic representation of the 2-compartment model for vitamin B-12 absorption with 2 simultaneous zero-order absorption processes is represented in Figure 2B. Active vitamin B-12 (HoloTC) was added as a significant covariate on the elimination coefficient ( $k$ ) and the plasma pool to tissue pool transfer coefficient ( $k_{12}$ ).

The observed plasma measurements were well predicted by the chosen model, as revealed by the simulation-based visual prediction check plot, goodness-of-fit plots, and residual distribution in Figure 2C, D and Supplemental Figure 6. The estimated population pharmacokinetic parameters are summarized in Table 2. Low residual variability (additive:  $2.22\text{e}^{-16}$ , proportional: 0.22) was observed, suggesting that most of the variability is explained by the model. Overall, the parameters were well estimated with good precision (relative standard error

$\leq 19\%$ ), which demonstrated the adequacy of the chosen model except for 2 parameters,  $V_{app}$  and  $k$ , for which the precision could not be computed by the tool. Further, low precision was observed for between-subject variability parameters that could be attributed to the distinctly high plasma appearance of tracer in one of the subjects, who had an elevated plasma vitamin B-12 concentration, thereby introducing a high variability in this small sample size ( $n = 4$ ). For the same subject, the model estimated a 125-fold higher elimination coefficient ( $k$ ) and a 7-fold lower plasma to tissue pool transfer coefficient ( $k_{12}$ ) in comparison to the population estimates. This emphasizes the strong association reported between tissue distribution of vitamin B-12 and its baseline concentrations (22). Most of the dose was absorbed in the first absorption phase ( $F_1 = 62\%$ ) over a period of 7.8 h immediately following dose administration. The remaining fraction was absorbed between 4.9 and 8.2 h after dose administration. The bioavailability ( $f_{\%}$ ) of [ $^{13}\text{C}$ ]-cyanocobalamin at the high dose (18.3  $\mu\text{g}$ ) ranged from 6% to 10% with a mean  $\pm$  SD value of  $7.6\% \pm 1.7\%$  (Table 3).

#### Pharmacokinetics of a low oral dose (2.3 $\mu\text{g}$ ) of [ $^{13}\text{C}$ ]-cyanocobalamin.

The anthropometric and biochemical characteristics of the study participants ( $n = 11$ , all males, including a repeat measurement of one of the subjects from the high-dose experiment) are provided in Table 1. The subjects had a BMI ranging from 18.5 to 25 kg/m<sup>2</sup> and vitamin B-12 of 104 to 310 pmol/L. Nine subjects had plasma vitamin B-12 concentrations in the normal range (>150 pmol/L), whereas 2 had lower vitamin B-12 (<150 pmol/L) concentrations. The mean plasma HoloTC concentration in the subjects was 36.8 pmol/L (Table 1). Their plasma methylmalonic acid and homocysteine concentrations were  $0.75 \pm 0.92$  and  $24.0 \pm 30.0$  ( $\mu\text{mol/L}$ , mean  $\pm$  SD), respectively; these were well above the reference range and are indicative of functional vitamin B-12 deficiency (23). The model described above (for the high-dose data) was used to fit the low-dose experimental data. No covariates were added to the model as none of the variables demonstrated any significant correlation with any of the random effects. Individual fits, final estimated parameters, and the goodness-of-fit plots for the low-dose data have been summarized in Supplemental Figure 7, Table 2, and Supplemental Figure 8, respectively. There was a reasonable concordance in the population parameter estimates for  $Tk_{01}$ ,  $F_1$ , and  $k_{21}$  between the 2 dosing regimens. A comparative analysis highlighted a higher elimination coefficient ( $k$ ), lower plasma pool to tissue pool transfer coefficient ( $k_{12}$ ), and an early initiation of a longer second absorption phase ( $Tlag_2$ ,  $Tk_{02}$ ) in the low-dose experiment, suggesting an association of these pharmacokinetic parameters with the dosage of oral B-12 supplementation. A high degree of between-subject variability was estimated for parameters such as the elimination coefficient ( $k$ , 44%), tissue pool to plasma pool transfer coefficient ( $k_{21}$ , 164%), and first-phase absorption fraction ( $F_1$ , 171%), suggesting a multifactorial basis for the large variability in the absorption and appearance of B-12. A convergence assessment of the model, with high- and low-dose data, produced satisfactory results with a median coefficient of variation of 16% and 23%, respectively, for population parameters estimated from 5 SAEM runs using random initial parameter values (Supplemental Figures 9–12).

**TABLE 2** Parameter estimates from the mathematical model for the concentration-time profiles from the high-dose ( $n = 4$ ; 2 males and 2 females) and low-dose ( $n = 14$ ; males) [ $^{13}\text{C}$ ]-cyanocobalamin experiment<sup>1</sup>

Parameter	High dose		Low dose	
	Estimate (% RSE)	% BSV (% RSE)	Estimate (% RSE)	% BSV (% RSE)
$Tk_{01}$ , h	7.82 (10.6)	2.3 (148)	7.62 (4.1)	5.36 (62.9)
$Tk_{02}$ , h	3.34 (11)	3.4 (264)	5.4 (17.6)	35 (44)
$F_1$ , %	0.62 (12.1)	31.5 (90.3)	0.578 (26.1)	171 (28.4)
$Tlag_2$ , h	4.92 (12.1)	8.4 (228)	3.39 (15.2)	41.4 (26.3)
$V_{app}$ , L	31 (NC)	3.5 (NC)	5.47 (23.4)	36.6 (38.7)
$k$ , $\text{h}^{-1}$	0.000352 (NC)	6.3 (214)	0.778 (36.5)	43.8 (59.6)
$k_{12}$ , $\text{h}^{-1}$	4.31 (18.8)	14.1 (93.6)	0.632 (42.7)	31.3 (77.7)
$k_{21}$ , $\text{h}^{-1}$	0.217 (15.8)	11.8 (189)	0.188 (114)	164 (86.8)
beta_k_Active_B-12 <sup>2</sup>	0.0377 (9.2)	—	—	—
beta_k <sub>12</sub> _Active_B-12 <sup>2</sup>	-0.0156 (16.7)	—	—	—
Error model parameters (residual variability)				
a (additive)	2.22 e <sup>-16</sup>	—	2.22 e <sup>-16</sup>	—
b (proportional)	0.218 (11.8)	—	0.241 (9.99)	—
BIC	161.22	—	34.84	—
Dose, $\mu\text{g}$	18.29 $\pm$ 0.90	—	2.29 $\pm$ 0.31	—
Bioavailability, $f\%$	7.6 $\pm$ 1.7	—	53.1 $\pm$ 18.1	—

<sup>1</sup> $n = 14$  includes data from the 3 low-dose experiments: initial low-dose experiment ( $n = 11$ ) and repeat measurement on ( $n = 3$ ) subjects after B-12 replenishment. BIC, Bayesian information criterion; BSV, between-subject variability;  $F_1$ , fraction of the bioavailable dose absorbed by the first zero-order mechanism;  $k$ , elimination rate constant;  $k_{12}$ , distribution rate constant from compartment 1 (plasma) to compartment 2 (peripheral tissues);  $k_{21}$ , distribution rate constant from compartment 2 (peripheral tissues) to compartment 1 (plasma); NC, not computed; RSE, relative standard error;  $Tk_{01}$ , duration of the first zero-order process;  $Tk_{02}$ , duration of the second zero-order process;  $Tlag_2$ , time delay before the start of the second zero-order absorption process;  $V_{app}$ , apparent volume of distribution.

<sup>2</sup>Covariates (active B-12; holotranscobalamin concentrations) were added only for the model describing high-dose data.

The low-dose kinetic model parameters showed that the bioavailability in healthy male subjects ( $n = 11$ ) with low to normal vitamin B-12 status ranged from 33.9% to 79%, with a mean  $\pm$  SD value of 46.2%  $\pm$  13% and CV of 28% (Table 4). The total plasma vitamin B-12 concentrations (measured by chemiluminescence) correlated significantly with baseline plasma unlabeled methylcobalamin (measured by mass spectrometry) concentrations ( $n = 11$ ,  $r = 0.86$ ,  $P = 0.0007$ ) and negatively correlated with plasma methylmalonic acid ( $n = 11$ ,  $r = -0.66$ ,  $P = 0.027$ ) and homocysteine concentrations ( $n = 11$ ,  $r = -0.61$ ,  $P = 0.046$ ). No significant correlations of plasma vitamin B-12 concentration with plasma HoloTC concentration or with vitamin B-12 bioavailability were observed.

#### Pharmacokinetics of a low oral dose (2.3 $\mu\text{g}$ ) of [ $^{13}\text{C}$ ]-cyanocobalamin after replenishment of stores in subjects with low vitamin B-12 status.

The pharmacokinetics of a low dose (2.3  $\mu\text{g}$ ) of [ $^{13}\text{C}$ ]-cyanocobalamin in male subjects ( $n = 3$ ; this was a repeat measurement for these subjects from the low-dose experiment) with low plasma HoloTC concentrations were studied after replenishing their body vitamin B-12 stores (2 wk after a single intramuscular injection of 1 mg hydroxocobalamin). Individual fits for the final model describing the absorption profile of subjects before and after replenishing their body vitamin B-12 stores are provided in Supplemental Figure 13. The replenishment of B-12 stores resulted in an improved percent (%) bioavailability (from 40.3  $\pm$  5.6 to 78.4  $\pm$  9.9, mean  $\pm$  SD; Supplemental Table 2). This was driven by a mean 13% reduction in the plasma pool to tissue pool transfer coefficient

( $k_{12}$ ), a 31% reduction in the elimination coefficient ( $k$ ) from the plasma pool, and a 5.4-fold increase in the tissue pool to plasma pool transfer coefficient ( $k_{21}$ ). Thus, the mean fractional bioavailability increased 1.9-fold after replenishing body B-12 stores. The plasma HoloTC concentration also increased significantly [5-fold; from 16.6  $\pm$  10.8 to 87.3  $\pm$  15.5 (pmol/L, mean  $\pm$  SD)] 2 wk after the intramuscular hydroxocobalamin injection.

#### Development of a potential clinical test for absorption.

Toward the development of a safe clinical diagnostic tool for bioavailability with minimal blood sampling, the bioavailability values were significantly and positively correlated with the plasma concentration of [ $^{13}\text{C}$ ]-methylcobalamin at 5, 6, and 7 h after the dose ( $n = 14$ ;  $\rho = 0.88$ , 0.64, and 0.69;  $P < 0.013$ ) administration. Therefore, these time points (between 5 and 7 h after the dose) can be considered a sampling window to define an index of bioavailability when considering this test as a clinical diagnostic tool.

#### Discussion

A stable isotope-based measurement of vitamin B-12 bioavailability has not been reported until now. Using *Salmonella typhimurium* and [ $^{13}\text{C}$ ]-ethanolamine as a carbon substrate, we biosynthesized a novel, stable isotope-labeled vitamin B-12, [ $^{13}\text{C}$ ]-cyanocobalamin, and characterized its chemical integrity and [ $^{13}\text{C}$ ]-incorporation before measuring its oral bioavailability in adult humans. This measurement was also made after the acute replenishment of stores in deficient subjects. With a mean oral



TABLE 3 Parameter estimates and bioavailability profiles in the high-dose [<sup>13</sup>C]-cyanocobalamin experiment<sup>1</sup>

ID	Age, y	Vitamin B-12, pmol/L	HoloTC, pmol/L	Methylcobalamin, pmol/L	T <sub>k01</sub> , h	T <sub>k02</sub> , h	F <sub>1</sub> , %	T <sub>lag2</sub> , h	V <sub>app</sub> , L	k, h <sup>-1</sup>	k <sub>12</sub> , h <sup>-1</sup>	k <sub>21</sub> , h <sup>-1</sup>	Dose, μg	Bioavailability (f <sub>0</sub> ), %
BA-HD-02	33	585.2	128.0	2343.4	7.9	3.3	0.5	4.6	31.1	0.044	0.6	0.2	19.4	9.8
BA-HD-14	23	152.8	20.9	421.8	7.8	3.3	0.7	5.0	31.2	0.001	3.5	0.2	17.5	8.1
BA-HD-15	30	178.6	27.2	422.2	7.8	3.4	0.6	4.8	30.6	0.001	2.4	0.2	18.5	6.5
BA-HD-16	26	160.1	15.5	299.8	7.8	3.4	0.7	5.1	31.1	0.001	3.7	0.2	17.7	6.0
Mean	28	269.2	47.9	871.8	7.82	3.35	0.61	4.86	31.01	0.012	2.52	0.22	18.3	7.6
SD	4.4	211.0	53.6	982.8	0.04	0.01	0.07	0.20	0.26	0.022	1.40	0.02	0.90	1.7

<sup>1</sup>F<sub>1</sub>, fraction of the bioavailable dose absorbed by the first zero-order mechanism; HoloTC, holotranscobalamin; k, elimination rate constant; k<sub>12</sub>, distribution rate constant from compartment 1 (plasma) to compartment 2 (peripheral tissues); k<sub>21</sub>, distribution rate constant from compartment 2 (peripheral tissues) to compartment 1 (plasma); T<sub>k01</sub>, duration of the first zero-order process; T<sub>k02</sub>, duration of the second zero-order process; T<sub>lag2</sub>, time delay before the start of the second zero-order absorption process; V<sub>app</sub>, apparent volume of distribution.

dose of 2.3 μg, which approximates the daily requirement, the average bioavailability was ~50%, similar to previous estimates of 60%, using crystalline [<sup>58</sup>Co]-cyanocobalamin (24–27). This was also concordant with the bioavailability reported from foods such as [<sup>14</sup>C]-vitamin B-12 fortified bread (28) and meat-based foods (27). With a higher dose of 18.3 μg, the mean bioavailability was lower at 7.6%, confirming the saturation of intestinal absorption mechanisms, in agreement with earlier observations (29, 30). This is underscored by the similar total bioavailable dose from the low-dose (1.3 ± 0.4 μg) and high-dose (1.4 ± 0.4 μg) protocols, which fall within the reported maximum absorptive capacity of 1.5–2.0 μg vitamin B-12 per meal (20). Currently, for defining the dietary requirement, vitamin B-12 bioavailability is assumed to be 40–50% for healthy adults with a normal gut, based on labeled vitamin B-12 studies from foods (11, 24, 27, 31–34). It is possible that at a very low vitamin B-12 intake, the bioavailability could be higher, but this is unlikely, since the bioavailability at doses of 0.8 to 2.6 μg has also been measured to be ~50–55% (28, 35). The assessment of bioavailability is also useful for defining the dose and route of administration of supplements in malabsorption-related vitamin B-12 deficiency (36) and for the evaluation of vitamin B-12 fortification concentrations.

The interindividual variability in bioavailability at low dose (CV 28%, resulting in a >2-fold difference between the minima and maxima) is important both for setting a dietary intake requirement and when considering the widespread deficiency of vitamin B-12. In part, this variability could be due to the effect of the existing vitamin B-12 in the body tissue pool, which affects the exchange of absorbed tracer between the plasma and tissue pools, as shown by the large variation in the transfer coefficients (k<sub>12</sub> and k<sub>21</sub>) and the elimination coefficient (k). The smaller the tissue pool, the greater the transfer of the absorbed tracer, resulting in a lower bioavailability estimate. This was borne out by the 1.9-fold increase in bioavailability after parenteral replenishment with 1 mg hydroxocobalamin in low vitamin B-12 status subjects, along with an anticipated decreased movement of tracer from the plasma to the tissue pool, increased tracer transfer into the plasma pool from the tissues, and a decrease in tracer elimination (k) from the plasma pool, possibly because of a lower need for (irreversible) tissue utilization. However, other factors like genetic variants could also be responsible for the high variability, since these are also known to influence vitamin B-12 bioavailability by altering the function of key proteins that are involved in either intestinal absorption or later transport, such as the fucosyltransferase (*FUT2* and *FUT6*), which is associated with susceptibility to *Helicobacter pylori* infections in the gut, B-12 transporters; haptocorrin and transcobalamin and the intestinal receptor for the intrinsic factor–vitamin B-12 complex, cubilin (*CUBN*) (37).

The kinetics of [<sup>13</sup>C]-cyanocobalamin were complex and described by a 2-compartment model. The existing knowledge about the kinetics of orally administered vitamin B-12 absorption is limited. Previously, Castelli et al. (38) compared different oral cyanocobalamin formulations at high doses using a simplified noncompartmental analysis in healthy subjects. The results from the present population pharmacokinetics approach provide significant insights into the absorption kinetics of orally administered vitamin B-12 in healthy subjects. The vitamin B-12 absorption process, which involves a carrier-mediated

TABLE 4 Parameter estimates and bioavailability profiles in the low-dose [<sup>13</sup>C]-cyanocobalamin experiment<sup>1</sup>

ID	Age, y	Vitamin B-12, pmol/L	HoloTC, pmol/L	Methylcobalamin, pmol/L	$T_{k01}$ , h	$T_{k02}$ , h	$F_1$ , %	$Tlag_2$ , h	$V_{app}$ , L	$k$ , h <sup>-1</sup>	$k_{12}$ , h <sup>-1</sup>	$k_{21}$ , h <sup>-1</sup>	Dose, µg	Bioavailability ( $f_{90}$ ), %
BA-02	33	178.6	58.7	308.7	7.6	3.8	0.1	3.9	7.2	0.8	0.7	0.4	2.2	43.3
BA-03	28	147.6	47.3	187.0	7.5	4.7	0.7	2.7	6.1	0.9	0.7	0.1	1.8	49.9
BA-04	24	104.1	5.0	92.9	7.6	5.5	0.5	6.0	6.4	1.0	0.7	0.0	2.0	39.5
BA-06	24	188.2	8.8	203.4	7.5	5.6	0.8	5.0	5.2	1.0	0.7	0.0	2.7	40.5
BA-07	44	186.0	26.4	181.6	7.6	5.2	0.7	2.3	3.1	1.1	0.7	0.1	3.1	35.1
BA-08	21	198.5	41.6	203.3	7.7	5.0	0.7	5.0	3.8	0.8	0.6	0.1	2.3	79.0
BA-09	26	173.4	63.6	177.8	7.6	6.6	0.2	2.4	6.4	1.0	0.7	0.1	2.1	36.6
BA-10	27	223.6	35.6	285.4	7.7	6.0	0.6	4.0	5.7	0.9	0.7	0.1	2.3	48.7
BA-11	21	273.8	58.5	301.2	7.1	3.7	0.6	3.0	5.0	1.4	0.7	0.0	2.2	56.0
BA-12	21	310.0	41	594.2	7.7	6.9	0.0	1.8	7.6	0.6	0.8	0.4	2.4	33.9
BA-13	26	179.3	18.4	161.9	7.5	6.1	0.6	2.8	5.6	0.8	0.6	0.1	2.4	46.2
Mean	26.8	196.6	36.8	245.2	7.6	5.4	0.5	3.5	6.1	0.9	0.7	0.1	2.3	46.2
SD	6.7	56.4	20.2	132.7	0.2	1.0	0.3	1.4	1.2	0.2	0.0	0.1	0.4	12.8

<sup>1</sup> $F_1$ , fraction of the bioavailable dose absorbed by the first zero-order mechanism; HoloTC, holotranscobalamin;  $k$ , elimination rate constant;  $k_{12}$ , distribution rate constant from compartment 1 (plasma) to compartment 2 (peripheral tissues);  $k_{21}$ , distribution rate constant from compartment 2 (peripheral tissues) to compartment 1 (plasma);  $T_{k01}$ , duration of the first zero-order process;  $T_{k02}$ , duration of the second zero-order process;  $Tlag_2$ , time delay before the start of the second zero-order absorption process;  $V_{app}$ , apparent volume of distribution.

transport in the ileum, was explained by a zero-order process with a constant transfer rate that was dependent on the capacity of the membrane carriers when provided at a concentration higher than the absorptive capacity. The plasma appearance of [<sup>13</sup>C]-methylcobalamin reached a peak between 5 and 8 h, similar to that reported earlier in [<sup>14</sup>C]-labeled vitamin B-12-based absorption studies in adults and the elderly (14, 28). However, the plasma appearance showed an earlier but smaller peak, ~3 h after the dose, and could be possibly due to passive absorption mechanism rather than by the intrinsic factor-mediated physiologically active cobalamin absorption mechanism in the ileum. A similar double-phase phenomenon following oral administration in fasted subjects has been reported previously (39). In the present study, using [<sup>13</sup>C]-cyanocobalamin, the variation in first phase absorption ( $F_1$ ) was high, possibly due to variable gastric emptying and small intestinal transit. In the fasted state, the 2-phase absorption process could be attributed to cyclical gastric emptying and variable gastrointestinal motility through the interdigestive migrating motility complex (IMMC) (40, 41). The pharmacokinetic model estimated the time lag before the second absorption phase ( $Tlag_2$ ) at 3.4 h in the low-dose experiment and 4.9 h in the high-dose experiment, which shows reasonable concordance with the mean IMMC cycling time in humans (112–230 min, SD: 58–70 min) (42). Water and dissolved substances are emptied fairly rapidly from the stomach (~40 min for 50% emptying) and can reach the cecum in 2–3 h (43), allowing for a combination of early passive absorption in the upper gastrointestinal tract (44, 45), along with an early active absorption from the fairly rapid entry of the water-based dose into the ileum.

Other noteworthy aspects included the observation that orally administered [<sup>13</sup>C]-cyanocobalamin was completely decyanated to [<sup>13</sup>C]-methylcobalamin, even with the high dose of 18.3 µg, in agreement with an earlier report (19). Our findings also suggest that the splanchnic decyanation is rapid, describing efficient cellular decyanase activity that enables the metabolic utilization of oral cyanocobalamin, possibly catalyzed by the cytosolic chaperone protein MMACHC (methylmalonic aciduria type C and homocystinuria), including methionine synthase reductase and novel reductase 1, which are ubiquitously expressed in most tissues (19, 46). In contrast, the oral administration of a dose of 27 µg cyanocobalamin per day in split doses has resulted in a significant plasma appearance of cyanocobalamin in 24 h (47), highlighting the need to ascertain the true decyanation capacity. There was also a reappearance of tracer, or an increase in the plasma [<sup>13</sup>C]-methylcobalamin concentrations, observed 10 h after the dose for most subjects, and could be result of enterohepatic circulation due to the ingestion of a light meal 7 h after the dose, where gallbladder emptying could result in secretion of absorbed tracer into the gut for reabsorption (48).

The labeling of the synthesized [<sup>13</sup>C]-cyanocobalamin was also noteworthy. *S. enterica* produces vitamin B-12 through δ-aminolevulinic acid (ALA) synthesis by the C<sub>4</sub> and C<sub>5</sub> pathways, similar to *Escherichia coli* (49–51). Two labeled carbons are conserved until δ-ALA synthesis, resulting in the incorporation of up to 16 [<sup>13</sup>C] into vitamin B-12 through the C<sub>5</sub> pathway, whereas in the C<sub>4</sub> pathway, due to the loss of 1 [<sup>13</sup>C] during the decarboxylation step, eventually the ALA molecule will contain only 1 [<sup>13</sup>C], thereby forming a porphobilinogen ring with 2 [<sup>13</sup>C] at each carboxylic acid group on the A (CH<sub>2</sub>COOH)

and P (CH<sub>2</sub>CH<sub>2</sub>COOH) sites of the corrin ring, explaining the incorporation of up to 7 [<sup>13</sup>C] in the tracer. The incorporation of more than a single [<sup>13</sup>C] is important in tracing the labeled moiety by HRAM-MS, as different metabolic forms of vitamin B-12 can give rise to doubly and triply charged species during in-source ionization.

The need for a safe clinical test of bioavailability has been highlighted earlier (26) in the investigation of vitamin B-12 deficiency, and the method described here meets that requirement. The CobaSorb test, based on an increment in the plasma HoloTC concentration following oral dosing with vitamin B-12, is somewhat limited since it cannot be used after supplementation (52). While the classical Schilling test uses an orally administered [<sup>57</sup>Co]-labeled vitamin B-12 followed by an intramuscular flushing dose of unlabeled vitamin B-12 and noninvasive but burdensome complete 24-h urine collection, the [<sup>14</sup>C]-labeled vitamin B-12 test, labeled at one particular atom of the dimethylbenzimidazole (DMB) moiety, poses a negligible radiation risk in comparison to [<sup>57</sup>Co] and is performed without a flushing dose of unlabeled vitamin B-12. It also requires very small volumes (<100 μL) of blood, urine, and fecal collection. Importantly, the labeling at the DMB moiety has revealed likely degradation or metabolism of the vitamin B-12 molecule in the gastrointestinal tract (14), which was not observed using [<sup>57</sup>Co]- or [<sup>58</sup>Co]-cobalamin. It is possible that such degradation would occur with the present [<sup>13</sup>C]-cobalamin, but this needs further evaluation, since the present evaluation was limited by the lack of urine and fecal collections. As such, the present method uses a safe stable isotope-labeled vitamin B-12 but needs serial blood sampling and can provide an index of bioavailability using timed plasma concentrations of [<sup>13</sup>C]-methylcobalamin between 5 and 7 h after the dose, and this needs further testing and validation. The lack of repeated measurements within subjects is a limitation toward the understanding of intraindividual variability. Further investigations with distinct instances of malabsorption, along with the inclusion of urine sampling for a true excretion term, and the examination of genetic covariates are warranted. Finally, a protocol for replenishment of vitamin B-12 status in deficient subjects will help improve the precision of the kinetic model underlying these bioavailability calculations.

We thank the subjects who participated in this study and the gift of the bacterial strain from the Department of Microbiology, UC Davis (Dr. John R. Roth). The contributions of D. B. Kashiraya and D. Vincent (senior laboratory technicians), Aneesia Varkey (research fellow), and Anika Andrea, M. S. Praveen, and D. Lobsang (research assistants) are acknowledged. We also thank Professors Tom Preston (Glasgow University, UK), Christopher Duggan (Boston Children's Hospital, USA), H. P. S. Sachdev (Sitaram Bhartia Institute of Science and Research, India), and Arpita Mukhopadhyay (St. John's Research Institute, India) for their critical review of the manuscript.

The authors' responsibilities were as follows—SD and AVK: designed the study; SD and ZS: performed the microbial biosynthesis and laboratory analyses with the supervision of AKM; SD and RMP: conducted animal and human studies, data collection, mass spectrometry analyses, and calculations; AS, KB, SD, and AVK: performed the pharmacokinetic modeling; SD and AVK: wrote the first draft of the manuscript with primary responsibility for the final content of the manuscript; all authors: critically reviewed and approved the final version of the manuscript.

Author disclosures: The authors report no conflicts of interest.

## References

- Zuckier LS, Chervu LR. Schilling evaluation of pernicious anemia: current status. *J Nucl Med* 1984;25:1032–9.
- Schilling RF. Intrinsic factor studies: II. The effect of gastric juice on the urinary excretion of radioactivity after the oral administration of radioactive vitamin B12. *J Lab Clin Med* 2004;144:268–72.
- Tata NIN Centre of Excellence in Public Health Nutrition Dashboard. Overview of food and nutrition in India [Internet]. Available from: <https://www.dashboard.nintata.res.in/#/dashboard/nutrient-intake>.
- EFSA Panel on Dietetic Products, Nutrition, and Allergies (NDA). Scientific opinion on Dietary Reference Values for cobalamin (vitamin B12). *EFSA J* 2015;13:4150. Available from: [www.efsa.europa.eu/efsajournal](http://www.efsa.europa.eu/efsajournal)
- Gonmei Z, Toteja GS. Micronutrient status of Indian population. *Indian J Med Res* 2018;148:511–21.
- Finkelstein JL, Kurpad AV, Thomas T, Srinivasan K, Duggan C. Vitamin B12 status in pregnant women and their infants in South India. *Eur J Clin Nutr* 2017;71:1046–53.
- Annibale B, Capurso G, Delle Fave G. Consequences of *Helicobacter pylori* infection on the absorption of micronutrients. *Dig Liver Dis* 2002;34:S72–7.
- Long AN, Atwell CL, Yoo W, Solomon SS. Vitamin B12 deficiency associated with concomitant metformin and proton pump inhibitor use. *Diabetes Care* 2012;35:e84.
- Green R. Vitamin B12 deficiency from the perspective of a practicing hematologist. *Blood* 2017;129:2603–11 [Internet]. Available from: <https://ashpublications.org/blood/article/129/19/2603/36140/Vitamin-B12-deficiency-from-the-perspective-of-a>.
- Baik HWW, Russell RMM. Vitamin B12 deficiency in the elderly. *Annu Rev Nutr* 1999;19:357–77.
- Watanabe F. Vitamin B 12 sources and bioavailability. *Exp Biol Med* 2007;232:1266–74.
- Carmel R. Malabsorption of food cobalamin. *Baillieres Clin Haematol* 1995;8:639–55.
- Carmel R. The disappearance of cobalamin absorption testing: a critical diagnostic loss. *J Nutr* 2007;137:2481–4.
- Carkeet C, Dueker SR, Lango J, Buchholz BA, Miller JW, Green R, Hammock BD, Roth JR, Anderson PJ. Human vitamin B12 absorption measurement by accelerator mass spectrometry using specifically labeled 14C-cobalamin. *Proc Natl Acad Sci* 2006;103:5694–9.
- Nexo E, Hoffmann-Lücke E. Holotranscobalamin, a marker of vitamin B-12 status: analytical aspects and clinical utility. *Am J Clin Nutr* 2011;94:359S–65S.
- Windelberg A, Årsæth O, Kvalheim G, Ueland PM. Automated assay for the determination of methylmalonic acid, total homocysteine, and related amino acids in human serum or plasma by means of methylchloroformate derivatization and gas chromatography-mass spectrometry. *Clin Chem* 2005;51:2103–9.
- Doets EL, in 't Veld PH, Szczecińska A, Dhonukshe-Rutten RAM, Cavelaars AEJM, van 't Veer P, Brzozowska A, de Groot LCPGM. Systematic review on daily vitamin B12 losses and bioavailability for deriving recommendations on vitamin B12 intake with the factorial approach. *Ann Nutr Metab* 2013;62:311–22.
- Reizenstein PG, Nyberg W. Intestinal absorption of liver-bound radiovitamin B12 in patients with pernicious anaemia and in controls. *Lancet* 1959;2:248–52.
- Kim J, Gherasim C, Banerjee R. Decyanation of vitamin B12 by a trafficking chaperone. *Proc Natl Acad Sci* 2008;105:14551–4.
- Scott JM. Bioavailability of vitamin B12. *Eur J Clin Nutr* 1997;51(Suppl 1):S49–53.
- Lindgren A, Kilander A, Bagge E, Nexø E. Holotranscobalamin—a sensitive marker of cobalamin malabsorption. *Eur J Clin Invest* 1999;29:321–9.
- Kornerup LS, Fedosov SN, Juul CB, Greibe E, Heegaard CW, Nexø E. Tissue distribution of oral vitamin B12 is influenced by B12 status and B12 form: an experimental study in rats. *Eur J Nutr* 2018;57:1459–69.
- Green R. Indicators for assessing folate and vitamin B-12 status and for monitoring the efficacy of intervention strategies. *Am J Clin Nutr* 2011;94:666S–72S.
- Food and Nutrition Board, Institute of Medicine Standing Committee on the Scientific Evaluation of Dietary Reference Intakes and Its Panel on Folate, Other B Vitamins and C. Vitamin B12In: Dietary reference intakes for thiamin, riboflavin, niacin, vitamin B6, folate, vitamin B12,

- pantothenic acid, biotin, and choline. Washington, DC: Institute of Medicine, National Academies Press; 1998. p. 196–305.
25. Allen LH. Causes of vitamin B 12 and folate deficiency. *Food Nutr Bull* 2008;29:S20–34.
  26. Green R, Allen LH, Bjørke-Monsen AL, Brito A, Guéant JL, Miller JW, Molloy AM, Nexo E, Stabler S, Toh BH, et al. Vitamin B12 deficiency. *Nat Rev Dis Prim* 2017;3:17040.
  27. Heyssel RM, Bozian RC, Darby WJ, Bell MC. Vitamin B12 turnover in man: the assimilation of vitamin B12 from natural foodstuff by man and estimates of minimal daily dietary requirements. *Am J Clin Nutr* 1966;18:176–84.
  28. Garrod MG, Buchholz BA, Miller JW, Haack KW, Green R, Allen LH. Vitamin B12 added as a fortificant to flour retains high bioavailability when baked in bread. *Nucl Instruments Methods Phys Res Sect B* 2019;438:136–40.
  29. Chanarin I. The megaloblastic anaemias. Oxford, UK: Blackwell Scientific; 1990.
  30. Adams JF, Ross SK, Mervyn L, Boddy K, King P. Absorption of cyanocobalamin, coenzyme B 12, methylcobalamin, and hydroxocobalamin at different dose levels. *Scand J Gastroenterol* 1971;6:249–52.
  31. Allen LH. Bioavailability of vitamin B12. *Int J Vitam Nutr Res* 2010;80:330–5.
  32. Doscherholmen A, McMahon J, Economon P. Vitamin B12 absorption from fish. *Exp Biol Med* 1981;167:480–4.
  33. Doscherholmen A, McMahon J, Ripley D. Vitamin B12 absorption from eggs. *Exp Biol Med* 1975;149:987–90.
  34. Doscherholmen A, McMahon J, Ripley D. Vitamin B12 assimilation from chicken meat. *Am J Clin Nutr* 1978;31:825–30.
  35. Garrod MG, Rossow HA, Calvert CC, Miller JW, Green R, Buchholz BA, Allen LH. 14C-cobalamin absorption from endogenously labeled chicken eggs assessed in humans using accelerator mass spectrometry. *Nutrients* 2019;11:2148.
  36. Berlin H, Berlin R, Brante G. Oral treatment of pernicious anemia with high doses of vitamin B12 without intrinsic factor. *Acta Med Scand* 1968;184:247–58.
  37. Nongmaithem SS, Joglekar CV, Krishnaveni GV, Sahariah SA, Ahmad M, Ramachandran S, Gandhi M, Chopra H, Pandit A, Potdar RD, et al. GWAS identifies population-specific new regulatory variants in FUT6 associated with plasma B12 concentrations in Indians. *Hum Mol Genet* 2017;26:2551–64.
  38. Castelli MC, Wong DF, Friedman K, Riley MGI. Pharmacokinetics of oral cyanocobalamin formulated with sodium N-[8-(2-hydroxybenzoyl)amino]caprylate (SNAC): an open-label, randomized, single-dose, parallel-group study in healthy male subjects. *Clin Ther* 2011;33:934–45.
  39. Doscherholmen A, Hagen PS. A dual mechanism of vitamin B12 plasma absorption. *J Clin Invest* 1957;36:1551–7.
  40. Yin OQP, Tomlinson B, Chow AHL, Chow MSS. A modified two-portion absorption model to describe double-peak absorption profiles of ranitidine. *Clin Pharmacokinet* 2003;42:179–92.
  41. Oberle RL, Amidon GL. The influence of variable gastric emptying and intestinal transit rates on the plasma level curve of cimetidine: an explanation for the double peak phenomenon. *J Pharmacokinet Biopharm* 1987;15:529–44.
  42. Dooley CP, Di Lorenzo C, Valenzuela JE. Variability of migrating motor complex in humans. *Dig Dis Sci* 1992;37:723–8.
  43. Malagelada JR, Robertson JS, Brown ML, Remington M, Duenes JA, Thomforde GM, Carryer PW. Intestinal transit of solid and liquid components of a meal in health. *Gastroenterology* 1984;87:1255–63.
  44. Herbert V. Absorption of vitamin B12 and folic acid. *Gastroenterology* 1968;54:110–5.
  45. Slot W, Merkus F, Van Deventer S, Tytgat G. Normalization of plasma vitamin B12 concentration by intranasal hydroxocobalamin in vitamin B12-deficient patients. *Gastroenterology* 1997;113:430–3.
  46. Lerner-Ellis JP, Tirone JC, Pawelek PD, Doré C, Atkinson JL, Watkins D, Morel CF, Fujiwara TM, Moras E, Hosack AR, et al. Identification of the gene responsible for methylmalonic aciduria and homocystinuria, cblC type. *Nat Genet* 2006;38:93–100.
  47. Hardlei TF, Mørkbak AL, Bor MV, Bailey LB, Hvas AM, Nexo E. Assessment of vitamin B12 absorption based on the accumulation of orally administered cyanocobalamin on transcobalamin. *Clin Chem* 2010;56:432–6.
  48. Teo NH, Scott JM, Neale G, Weir DG. Effect of bile on vitamin B12 absorption. *BMJ* 1980;281:831–3.
  49. Zhang L, Chen J, Chen N, Sun J, Zheng P, Ma Y. Cloning of two 5-aminolevulinic acid synthase isozymes HemA and HemO from *Rhodospseudomonas palustris* with favorable characteristics for 5-aminolevulinic acid production. *Biotechnol Lett* 2013;35:763–8.
  50. Kang Z, Wang Y, Gu P, Wang Q, Qi Q. Engineering *Escherichia coli* for efficient production of 5-aminolevulinic acid from glucose. *Metab Eng* 2011;13:492–8.
  51. Fang H, Kang J, Zhang D. Microbial production of vitamin B12: a review and future perspectives. *Microb Cell Fact* 2017;16:15.
  52. Hvas AM, Mørkbak AL, Hardlei TF, Nexo E. The vitamin B12 absorption test, CobaSorb, identifies patients not requiring vitamin B12 injection therapy. *Scand J Clin Lab Invest* 2011;71:432–8.